Temperature Analysis for the Linear Cell in the Vapor Deposition Process

Jongwook Choi*, Sungcho Kim, Jeongsoo Kim
School of Mechanical and Automotive Engineering, Sunchon National University, Suncheon, Jeonnam 540-742, Korea

The OLED (Organic Light Emitting Diodes) display recently used for the information indicating device has many advantages over the LCD (Liquid Crystal Display), and its demand will be increased highly. The linear cell should be designed carefully considering the uniformity of thin film on the substrate. Its design needs to compute the temperature field analytically because the uniformity for the thin film thickness depends on the temperature distribution of the source (organic material). In the present study, the design of the linear cell will be modified or improved on the basis of the temperature profiles obtained for the simplified linear cell. The temperature distributions are numerically calculated through the STAR-CD program, and the grids are generated by means of the ICEM CFD program. As the results of the simplified linear cell, the temperature deviation was shown in the parabolic form among the both ends and the center of the source. In order to reduce the temperature deviation, the configuration of the rectangular ends of the crucible was modified to the circular type. In consequence, the uniform temperature is maintained in the range of about 90 percent length of the source. It is expected that the present methods and results on the temperature analysis can be very useful to manufacture the vapor deposition device.

Key Words: OLED (Organic Light Emitting Diodes), Linear Cell, Uniformity of Thin Film, Vapor Deposition, Radiative Heat Transfer

1. Introduction

The display device in the information technology plays an important part in the information society of the 21st century, because the words or the images need to be transmitted freely to other people regardless of the time and the space. The CRT (Cathode Ray Tube) is on the way to make room for the FPD (Flat Panel Display) device in the field of the information display screen. The LCD (Liquid Crystal Display), one of the FPD's, has the merits of the thin thickness, the light weight, and the low power consumption in comparison with the CRT's. However, the LCD requires the light source from the back because it does not emit light in itself, and has the technical limits for the brightness, the contrast, the view angle, the scale and so on. On the other hand, the OLED (Organic Light Emitting Diodes) display has been researched and developed constantly since there are many strong points such as the low-voltage drive, the luminescence in itself, the wide view angle, the fast response, etc (Tang et al., 1989; Kido et al., 1994; Hamada et al., 1995; Tokito et al., 1995; Granström and Inganäs, 1996). This display already began to be employed for the outside panel of a mobile phone, and its demand will be gradually increased because its application is closely related to the small-sized display for the PDA (Personal Digital Assistants) the digital camera, the digital camcorder, etc.

* Corresponding Author,
E-mail : choijw99@sunchon.ac.kr
TEL : +82-61-750-3826; **FAX** : +82-61-753-3962
School of Mechanical and Automotive Engineering, Sunchon National University, Suncheon, Jeonnam 540-742, Korea. (Manuscript **Received** October 1, 2004; **Revised** May 4, 2005)

The OLED emits the light with the specific wavelength generated by the exciton energy, where the exciton is formed by the recombination of the electron and the hole injected into the cathode and the anode in the organic thin film. Since the phenomenon was found by Pope in 1963, the OLED has been studied using the mono-molecule (Tang and VanSlyke, 1987) and the polymers (Burroughes et al., 1990). Its structure is composed of the various components such as anode, HIL (Hole Injection Layer), HTL (Hole Transport Layer), EML (Emitting Layer), HBL (Hole Blocking Layer), ETL (Electron Transport Layer), EIL (Electron Injection Layer), and cathode. The thin film layers can be formed by the evaporation method in the vacuum state. In 1857, Faraday suggested the method generally used for manufacturing the thin film. This process is summarized like that the evaporated particles are deposited on the substrate after the metal, the compound or the alloy is evaporated or sublimated by heating in the vacuum condition. The physical steps for forming the thin film are the followings ; (1) The phase transition to the vapor state by evaporating the organic material, (2) The movement of atom or molecule from the source to the substrate, (3) The condensation of atom or molecule on the substrate, (4) The rearrangement of the particles on the substrate by the bonding strength.

The point cell (Choi et al., 2004 ; Smith, 1994) has widely been used in the vapor deposition in the vacuum due to the simple mechanism and the uniformity of thin film. However, the area of the substrate is restricted within narrow limits in the point cell. Therefore, the new type cell, e.g. the linear cell, has been required for the large-scaled display. The linear cell is noteworthy because it can be applied to manufacturing the large-scaled OLED display. In addition, it has merits of decreasing the consumption of organic material as well as the size of the vacuumed deposition device since the substrate can be approached near to the cell.

First of all, the uniformity of thin film, depending on the temperature distribution, should be considered in the vapor deposition process in the vacuum to design the linear cell. In this work, after the temperature field is computationally analyzed for the simplified linear cell model, the configuration of linear cell will be modified to improve the temperature characteristics by referring to those results. Then the temperature distribution is verified for the modified linear cell. The STAR-CD program (STAR-CD User Guide, 2001) and the ICEM CFD program (ICEM CFD Reference Manual, 2000) are utilized in the temperature analysis and in the grid generation, respectively.

2. Simplified Linear Cell

2.1 Design for the simplified linear cell

The conception of the linear cell for the substrate of 42 inch (730 mm×920 mm) is shown in Fig. 1. The crucible dimension is 920 mm×40 mm×100 mm, and the wall thickness is 10 mm. The crucible capacity is about 1,100 mm^3 considering the charging rate of 70 percent of the source. The source is sublimated by heating in the distribution of the cosine function (Smith, 1994). The heated source is deposited on the moving substrate in the vacuum chamber. The thickness of thin film on the ends of substrate is thinner than that of thin film on the center of substrate because the quantity of the overlapped source is small in the ends figured in Fig. 2. Therefore, the length of the crucible should be made longer than that of the substrate.

The simplified linear cell is designated in Fig. 3 to calculate the temperature distribution, on which the uniformity of thin film depends in the

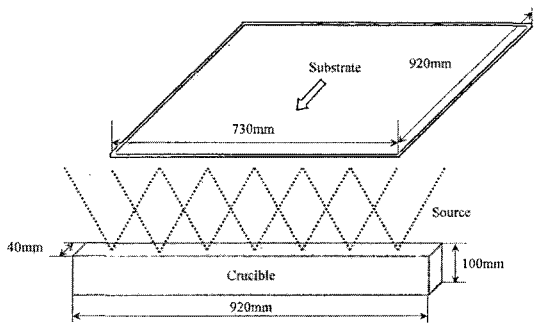

Fig. 1 Conception of the linear cell

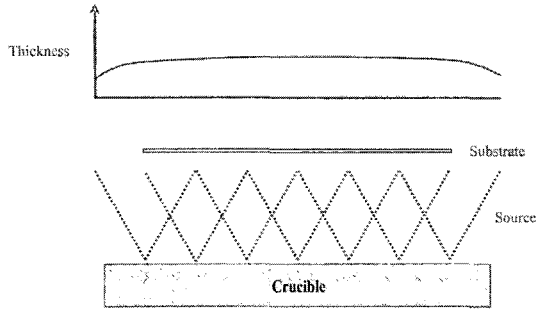

Fig. 2 Thickness of thin film on the substrate

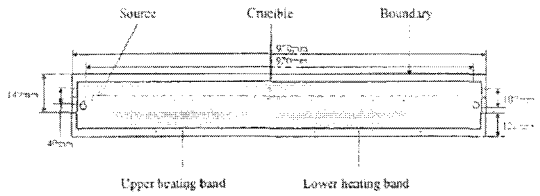

Fig. 3 Configuration and dimensions for the simplified linear cell

linear cell. The linear cell consists of the crucible, the source, and the two heating bands. The dimensions of the crucible and the boundary are also shown in Fig. 3. And the dimensions of the source and the heating band are 900 mm×20 mm×63 mm and 940 mm×80 mm×40 mm, respectively. The upper heating band plays a role in heating the upper parts of the source and the crucible. The high temperature of the upper crucible can prevent the source from being deposited on the crucible, and assists to deposit safely the source on the substrate. If the temperature of the upper crucible is lower than that of the sublimated source, the clogging phenomenon can appear in the upper crucible. The clogging is that the source is gradually deposited on the exit surface of the crucible and thus the crucible is clogged. The quantity of the sublimated source can be easily controlled with the fast response time by the heat flux of the upper heating band because the lower heating band plays a role for preheating the lower source with the low value of the heat conductivity.

2.2 Grid generation and boundary conditions

The geometric data for the simplified linear cell are saved in the IGES format for the gird generation. The grids are generated using the ICEM CFD program. The grids are the hexa mesh in type, and its total number is 45,056. The computational domain can be divided into a fluid region and two solid ones. The radiant heat from the heating bands is transferred into the fluid region of vacuum state, and the heat into two solid regions composed of the crucible and the source. The overlapped grids for the crucible and the source should be removed in the computational domain. The grids for the heating bands are not required in the calculated domain.

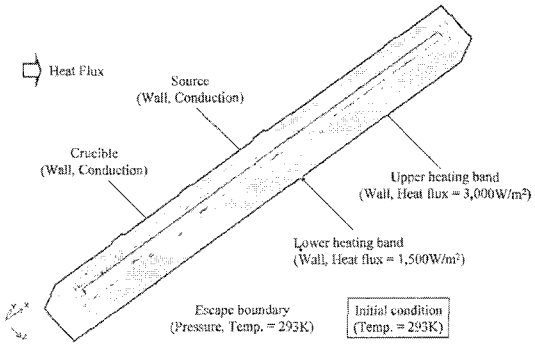

Fig. 4 Boundary conditions for the simplified linear cell

The boundary conditions for the simplified linear cell are shown in Fig. 4. The conduction boundary conditions are assigned to the crucible and source. Referring the physical properties, the values of heat flux for the upper and the lower heating bands are set to 3,000 W/m^2 and 1,500 W/m^2, respectively. The heat flux of the upper heating band is alloted to the higher value than that of the lower heating band to prevent the clogging. The ambient temperature of 293K is fixed at the escape boundary, and the initial temperature is also the very same.

2.3 Temperature analysis

The grids and the boundary conditions generated in the ICEM CFD program are utilized as the input data of the STAR-CD one. The numerical procedure for the temperature analysis using the STAR-CD program is shown in Fig. 5. Physically, the heat conductivity in the fluid region

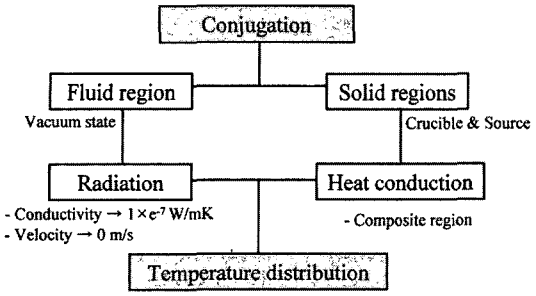

Fig. 5 Numerical procedure for temperature analysis

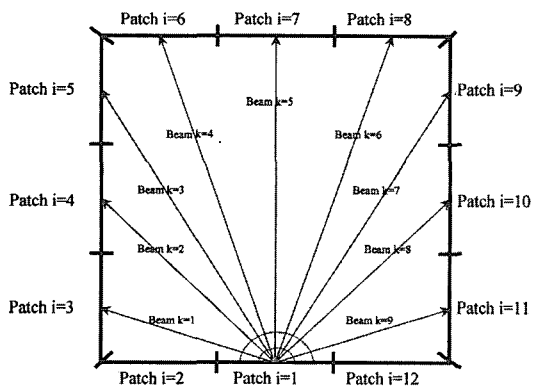

Fig. 6 Illustration of the patch and beam definitions

is assigned to a very small value of 1.0×10^{-7} W/mK and the flow velocity is set to 0 m/s. This conductivity is used for the analysis of radiative heat transfer in the vacuum state using the STAR-CD program (STAR-CD Tutorial, 2001).

The setup for the patches and the beams is required to analyze the radiative heat transfer. The beams radiate on the patches as described in Fig. 6, and the characteristic length of the patch is set to 20 mm. The number of patches and beams per patch are assigned to 3,182 and 10,000, respectively. The view factor F_{ij} between patches i and j is the fraction of the total radiation leaving surface i which is intercepted by j, and the equation can be expressed like $F_{ij}=\sum_{k=1}^{N_{L,i}}\alpha_k f_{ij}$, where $N_{L,i}$ is the total number of beams for the patch i, the coefficient α_k is equal to 1 if the beam strikes j or to zero otherwise, and f_{ij} is the view factor for a single beam emanating from the centroid of a patch, and deduced from the area intercepted on the unit hemisphere (STAR-CD Methodology, 2001). All materials in the linear cell are assumed as the gray bodies. The emissivities of the crucible (Al_2O_3) and the heating bands (SST) are set to 0.69 and 0.19, respectively (Incropera and DeWitt, 2002).

Table 1 Properties of the materials

Meterial	Density (kg/m^3)	Specific heat (J/kgK)	Conductivity (W/mK)
Fiuid	1.205	1,006	1.0×10^{-7}
Solid (Crucible)	3,960	850	30
Solid (Souree)	105	1,400	0.35

The heat conduction equation is used for obtaining the temperature in the crucible and the source. The temperature is calculated in the composite region considering each material with the different properties. The values of the density, the specific heat, and the conductivity for the materials are arranged in Table 1.

The velocities and pressure in the fluid region is not solved using the continuity and the momentum equations owing to the vacuum state. The only temperature is calculated with implicit algorithm by the energy equation. The upwind differencing scheme is used for numerical analysis. Finally, the temperature distributions are obtained at t=1,200, t=2,400, t=3,600, t=7,200, and the steady state, respectively.

2.4 Results and discussion

The temperature distribution of the source in the linear cell is closely related to the uniformity of thin film. Therefore, the analysis is focused on the temperature distribution only in the source. The temperature distributions on the source surface in the front view according to the elapsed time are plotted in Fig. 7. The temperature at the upper ends is higher than that at the center part because of the geometric characteristics of the crucible corner. The overall temperature is increased with time, and its distribution tends to be regular as time elapses. However, the source can be non-uniformly sublimated toward the substrate due to the temperature deviation.

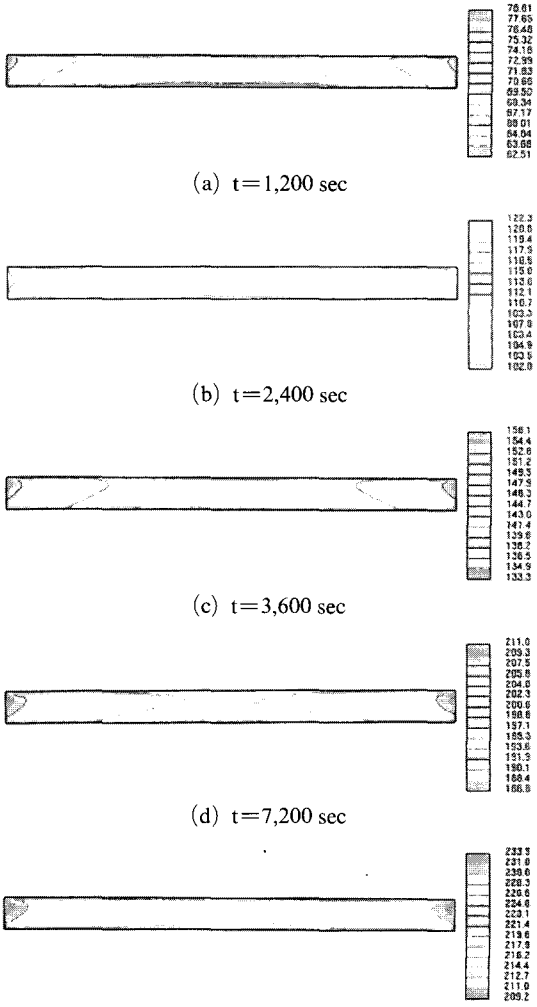

(a) t=1,200 sec

(b) t=2,400 sec

(c) t=3,600 sec

(d) t=7,200 sec

(e) steady state

Fig. 7 Temperature distribution on the source surface (front view)

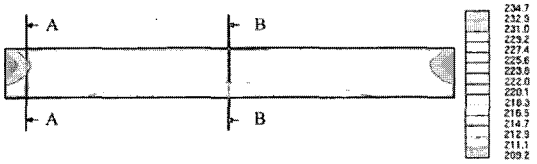

Fig. 8 Temperature distribution on the crucible surface (front view) (steady state, A-A : 5% position of the crucible length from the left end, B-B : the crucible center)

The temperature distribution on the crucible surface in Fig. 8 is similar to that on the source surface shown in Fig. 7(e) because the conductivity of the crucible is good. Fig. 9 shows the temperature distribution at the sections of the crucible and source. The positions of the section A-A and B-B are the 5 percent on the direction of the crucible length and its center, respectively (see Fig. 8). The tendencies of the temperature distribution are similar each other at the section A-A and B-B. However the overall temperature at the section A-A is higher than that at the section B-B because the radiative heat flux is large in the corner. The temperature of the upper crucible is higher than that of the lower one because the heat fluxes of the upper and lower heating bands are 3,000 W/m^2 and 1,500 W/m^2, respectively. On the other hand, the temperature of the upper source is relatively low as the escape boundary condition is 293K. The temperature distribution in other parts of the source seems to be similar to that in the crucible.

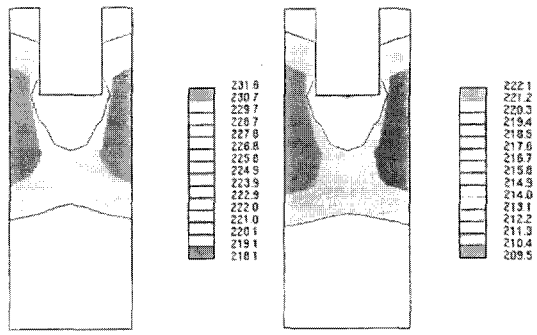

(a) Section A-A (b) Section B-B

Fig. 9 Temperature distribution at the sections (steady state)

3. Modified Linear cell

3.1 Design for the modified linear cell

As a result of the temperature analysis in the simplified linear cell, the temperature deviation was shown on the direction of length. The cause of the temperature deviation is that the incident area of the ends is larger than that of the center and also the heat of the ends flows into the center of the source. This temperature distribution can cause the thin film thickness not to be uniform in the vacuumed deposition process.

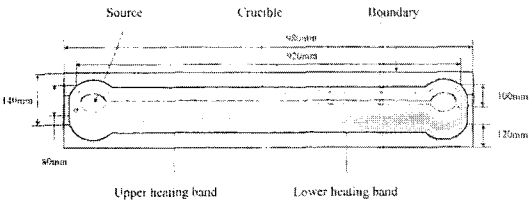

Fig. 10 Configuration for the modified linear cell

To improve the uniformity of thin film, the configuration of the ends for the crucible is modified to the circular type as designed in Fig. 10. The shapes of the heating bands and the source are also modified together with the crucible appearance. The dimensions of the crucible and the boundary are shown in Fig. 10. And the dimensions of the source and the heating band are 900 mm×20 mm×63 mm (diameter 60 mm) and 960 mm×80 mm×40 mm (diameter 120 mm), respectively. The modified geometry of the source plays an important part in blocking the heat flux moving from the ends to the center as the heat capacity increases in the ends.

3.2 Grid generation and temperature analysis

The methods of the grid generation and temperature analysis are similar to those for the simplified linear cell. The boundary conditions in the modified linear cell are described in Fig. 11. The number of grids and patches are 156,136 and 3,744, respectively, and the characteristic length of patch is 20 mm. The properties are all the same values adopted in the simplified linear cell.

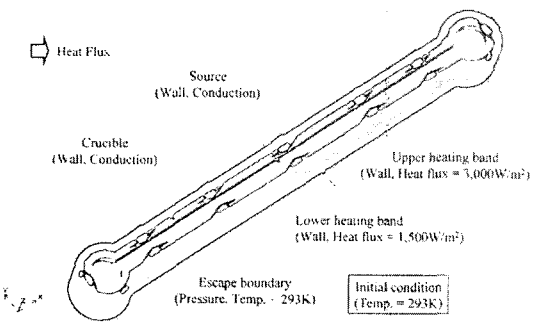

Fig. 11 Boundary conditions for the modified linear cell

3.3 Results and discussion

The temperature distributions on the source surface in the front view are shown in Fig. 12 at t=1,200, 2,400, 3,600, 7,200 sec, and the steady state, respectively. The tendency of temperature distribution is similar to that of the simplified linear cell at t=1,200 sec, that is, the temperature at the ends is higher than that at the center. However, the temperature deviation on the direction of the source length decreases with time. The temperature distribution is almost constant at the upper source except the ends as known in Fig. 12(e). The heat flux of the ends scarcely affect the

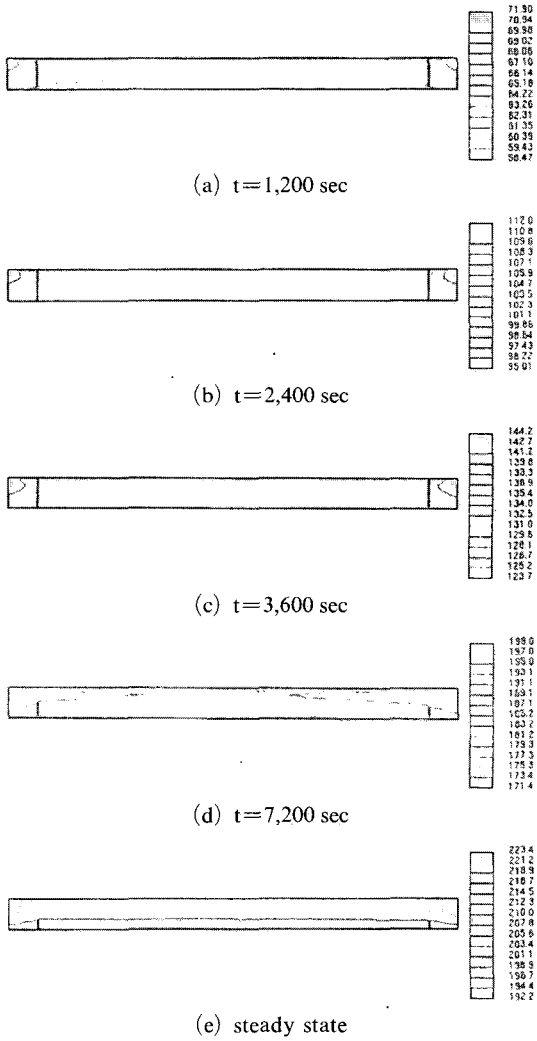

(a) t=1,200 sec

(b) t=2,400 sec

(c) t=3,600 sec

(d) t=7,200 sec

(e) steady state

Fig. 12 Temperature distribution on the source surface (front view)

center temperature of the source because of the increased heat capacity of the ends. Therefore, the temperature deviation is reduced on the source surface. The temperature distribution on the crucible surface at the steady state can be found in Fig. 13, and the temperature deviation is certainly decreased in comparison with the results of the simplified linear cell in Fig. 8. The temperature distribution at the two sections of the crucible and source is depicted in Fig. 14, and the tendency of temperature distribution is similar to that of the simplified linear cell.

The variations of non-dimensional temperature with time are given in Fig. 15 along the length on the source surface at both the simplified linear cell and the modified linear cell. Where, non-dimensional temperature = (temperature − min. temperature) / (max. temperature − min. temperature). The comparative position is the top edge of the source surface at t=1,200, 2,400, 3,600, 7,200 sec and the steady state, respectively. For the simplified linear cell, the temperature

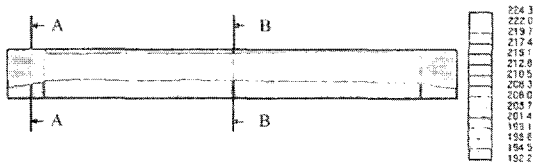

Fig. 13 Temperature distribution on the crucible surface (front view) (steady state, A-A : 5% position of the crucible length from the left end, B-B : the crucible center)

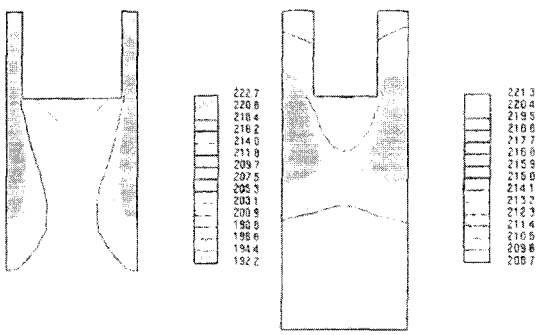

(a) Section A-A (b) Section B-B

Fig. 14 Temperature distribution at the sections (steady state)

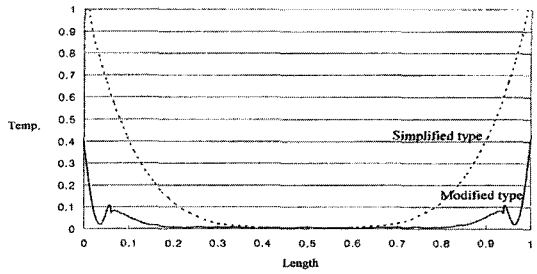

(a) t=1,200 sec

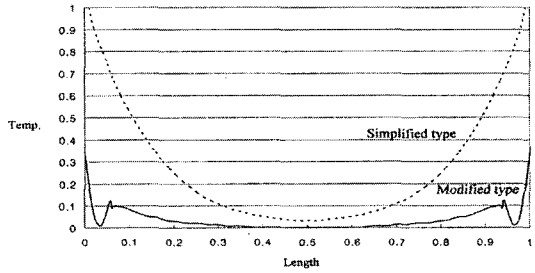

(b) t=2,400 sec

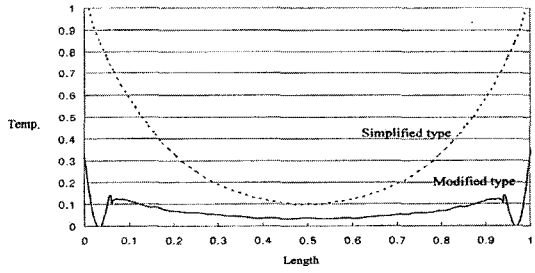

(c) t=3,600 sec

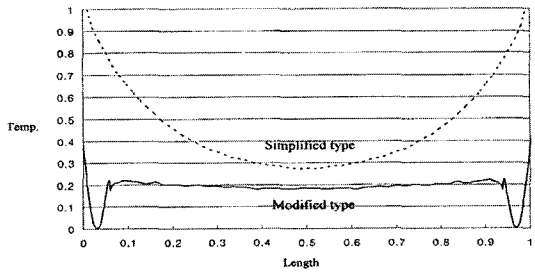

(d) t=7,200 sec

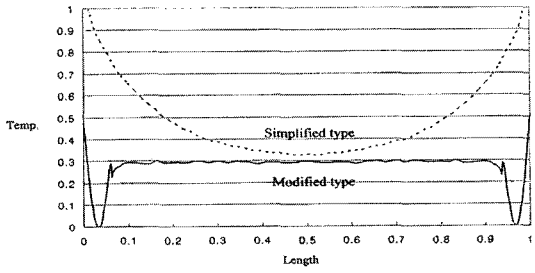

(e) steady state

Fig. 15 Variations of non-dimensional temperature with length on the source surface

curve is parabolic in the direction of the source length. That is, the temperature increases toward the ends, and it decreases near the center. This temperature distribution tends to be maintained until the steady state. For the modified linear cell, there are the temperature deviations at the center part as shown in Fig. 15(a)-(c), however the temperature is not nearly changed over the range of about 90 percent of the length except the ends at t=7,200 sec and the steady state as figured in Fig. 15(d)-(e). The source in the modified linear cell is expected to be sublimated uniformly at the steady state due to these temperature distributions.

4. Conclusions

The uniformity of thin film on the substrate should be considered to design the linear cell for manufacturing the large-scale OLED display. The uniformity depends on the temperature distribution in the linear cell. Therefore, the temperature distribution needs to be analyzed for designing linear cell. In the paper, the temperature distribution is calculated after the simplified linear cell is designed. As the result, the variation curve for the temperature on the direction of the length on the source surface is found as the parabolic type, because the incident area at the ends is larger than that at the crucible center and also the heat flux at the ends flows into the source center. To reduce the temperature deviation, the configuration at the ends of the crucible is modified to the circular type. The temperature distribution in the modified linear cell is almost constant at the center part in comparison with the results of the simplified linear cell. That is, the non-dimensional temperature is uniform in the range of about 90 percent over the source length. The circular ends of the crucible play an important part in blocking the heat flux flow from the ends to the center. As the heat capacity increases due to the circular geometry in the ends, the amount of heat flux gets decreased toward the center. The configuration and temperature results for the modified linear cell can be available to apply to manufacturing the vacuumed deposition device. In the future study, the temperature will be calculated according to the gap between the heat bands and the ends of crucible and to heat flux in the heat bands divided by two regions. The temperature distributions will also be solved for the linear cell with other components such as the water jacket, the outer case, the heating wires and so on. Finally, the optimum design of the linear cell will be found considering the temperature results.

Acknowledgments

This work was supported by the Korea Research Foundation Grant funded by Korean Government (MOEHRD) (R08-2003-000-10487-0)

References

Burroughes, J. H., Bradley, D. D. C., Brown, A. R., Marks, R. N., Maackay, K., Friend, R. H., Burns, P. L. and Holmes, A. B., 1990, "Light-Emitting Diodes based on Conjugated Polymers," *Nature*, Vol. 347, pp. 539~541.

Choi, J. W., Kim, S. C. and Jung, H., 2004, "Temperature Analysis for the Point-Cell Source in the Vapor Deposition Process," *KSME International Journal*, Vol. 18, No. 9, pp. 1680~1688.

Granström, M. and Inganäs, 1996, "White Light Emission from a Polymer Blend Emitting Diode," *Applied Physics Letter*, Vol. 68, No. 2, pp. 147~149.

Hamada, Y., Sano, T., Shibata, K. and Kuroki, K., 1995, "Influence of the Emission Site on the Running Durability of Organic Electroluminescent Devices," *Japanese Journal of Applied Physics*, Vol. 34, pp. L824~L826.

ICEM CFD Reference Manual (version 4.2), 2000, ICEM Engineering.

Incropera, F. P. and DeWitt, D. P., 2002, *Fundamentals of Heat and Mass Transfer*, John Wiley & Sons Inc., pp. 903~967.

Kido, J., Hongawa, K., Okuyama, K. and Nagai, K., 1994, "White Light-Emitting Organic Electroluminescent Devices using the Poly (N-Vinylcarbazole) Emitter Layer doped with Three Fluorescent Dyes," *Applied Physics Letters*, Vol.

64, No. 7, pp. 815~817.

Smith, D. L., 1994, *Thin-Film Deposition Principles and Practice*, McGraw-Hill, pp. 63~118.

STAR-CD Methodology (version 3.15), 2001, Computational Dynamics Limited, chap. 9.

STAR-CD Tutorials (version 3.15), 2001, Computational Dynamics Limited, chap. 12.

STAR-CD User Guide (version 3.15), 2001, Computational Dynamics Limited.

Tang, C. W. and VanSlyke, S. A., 1987, "Organic Electroluminescent Diodes," *Applied Physics Letter*, Vol. 51, No. 12, pp. 913~915.

Tang, C. W., VanSlyke, S. A. and Chen, C. H., 1989, "Electroluminescence of Doped Organic Thin Films," *Journal of Applied Physics*, Vol. 65, No. 9, pp. 3610~3616.

Tokito, S., Takata, J. and Taga, Y., 1995, "Organic/Inorganic Superlattices with Ordered Organic Layers," *Journal of Applied Physics*, Vol. 77, No. 5, pp .1985~1989.